# Parallel ion strings in linear multipole traps

M. Marciante,* C. Champenois, J. Pedregosa-Gutierrez, A. Calisti, and M. Knoop
*Physique des Interactions Ioniques et Moléculaires, UMR 6633 CNRS et Aix-Marseille Université, Centre de Saint Jérôme, Case C21, 13397 Marseille Cedex 20, France*
(Dated: March 8, 2011)

Additional radio-frequency (rf) potentials applied to linear multipole traps create extra field nodes in the radial plane which allow to confine single ions, or strings of ions, in totally rf field-free regions. The number of nodes depends on the order of the applied multipole potentials and their relative distance can be easily tuned by the amplitude variation of the applied voltages. Simulations using molecular dynamics show that strings of ions can be laser cooled down to the Doppler limit in all directions of space. Once cooled, organized systems can be moved with very limited heating, even if the cooling process is turned off.

Radio-frequency (rf) traps are very useful tools for a wide range of research interests such as high resolution spectroscopy [1], frequency standards [2], quantum information processing [3] and quantum simulations [4]. The ability to trap and cool atomic or molecular species in a well defined manner allows to control and study the quantum behaviour of these systems. Most experiments require a totally perturbation-free dynamics of the confined ions, and the micro-motion due to the rf trapping field can sometimes be a disturbing factor. In these cases, cold ions are confined in a string configuration along the longitudinal axis of a linear quadrupole trap, where the rf field vanishes. For a number of applications, in particular in quantum logic and quantum simulations [3, 4], it could be desirable to create more sites inside a trap where the ions do not undergo the rf parametric excitation. Linear traps of higher order, here called multipole traps, offer larger regions of low rf electric fields [5] which allow to trap large samples with a reduced driven micromotion, as compared to the same sample trapped in a linear quadrupole trap [6]. Local minima can be induced in the trapping potential by adding static voltages to these multipole rf voltages [7, 8] but the ions then undergo a rf driven motion which is detrimental when very low temperatures need to be reached. The superimposition of a lower order rf field onto the main trapping field generates minima to the trapping potential where the rf field is nulled. In such a configuration and depending on their number, the ions can settle in each minimum as individual ions or as parallel strings of ions expanding in the axial direction. Due to the absence of a local rf electric field, laser cooling can reduce the temperature of the ions as low as for a chain of ions in a quadrupole trap.

In this letter we first give an example of principle of the proposed method by combining a quadrupole potential with the potential created by a linear octupole trap. To demonstrate how to reach the Doppler limit by Doppler laser cooling we use molecular dynamics (m.d.) simulations of a 10-ion system, in a double line configuration. In a second part, we discuss the general case of two combined rf potentials of different order. In these two parts, we assume an ideal electric field for each superimposed rf field. In the third part of this letter, the effect of a non-ideal geometry to generate the lowest order rf field [9] is taken into account by combining m.d. simulations with an analytic fit of the actual electric field. This analysis shows that, providing an extra voltage which compensates for the imperfections of the electric fields, the same properties are observed and that our proposal still holds.

First, we describe the principle of the creation of extra rf field-free minima within the linear octupole trap geometry. In order to create additional nodes in the rf electric field, a rf quadrupole potential, with identical phase and frequency as the octupole potential, is superimposed onto the former. By the superposition theorem, the resulting rf electric potential $\Phi_{\rm rf}$ in the radial plane is given by

$$\Phi_{\rm rf} = \Phi_{8\rm rf} + \Phi_{4\rm rf}, \tag{1}$$

where the expression of the $2k$-pole electric potentials $\Phi_{(2k)\rm rf}$ using the polar coordinates (see Fig. 1) can be approximated by [5]:

$$\Phi_{(2k)\rm rf}(\mathcal{R},\phi,t) = -V_{2k}\mathcal{R}^k \cos(k\phi)\cos(\Omega t) \tag{2}$$

with $\Omega$ and $V_{2k}$ respectively the frequency and the amplitude of the applied rf potentials, and $\mathcal{R} = r/r_0$ the relative distance to the trap center, scaled to the inner radius of the trap $r_0$. The components of the electric field $\vec{E} = -\vec{\nabla}\Phi_{\rm rf}$ are:

$$E_r = +\frac{2}{r_0}\left[2V_8\mathcal{R}^3\cos(4\phi) + V_4\mathcal{R}\cos(2\phi)\right]\cos(\Omega t), \tag{3}$$

$$E_\phi = -\frac{2}{r_0}\left[2V_8\mathcal{R}^3\sin(4\phi) + V_4\mathcal{R}\sin(2\phi)\right]\cos(\Omega t). \tag{4}$$

With our choice of initial phase and frame reference (sketched on Fig. 1), it is straightforward from Eq. 4 that $E_\phi$ can be cancelled for any direction defined by $\phi_n = n\pi/2$, with $n \in \mathbb{Z}$. The relative variation of the cosines in Eq. 3 makes then possible a total rf field cancellation at the relative radial positions $\mathcal{R}_{0\rm f}$ for $\phi_{\pm1} = \pm\pi/2$ (the $y$-axis in our case, see Fig. 1). This relative radial position depends on the ratio of the two rf voltages as :

$$\mathcal{R}_{0\rm f}^2 = V_4/2V_8. \tag{5}$$

*mathieu.marciante@etu.univ-provence.fr

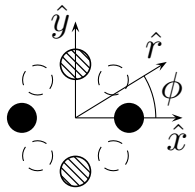


FIG. 1. Connection of a quadrupole rf electric potential onto the electrodes of an octupolar trap. Black and hatched rods show the different polarities of the applied $-V_4$ and $+V_4$ potentials respectively, at time $t = 0$ s. The broken line rods are only connected to the octupolar potential .

In the adiabatic approximation, where the rf period is much smaller than the time scale of the motion induced by the spatial variation of the electric field amplitude (the so-called macro-motion) [10], the dynamics of an ion of charge $q_e$ and mass $m$ inside the trap can be understood using the pseudopotential (psp) $\Psi$, which results from the time-average of the rf electric field $\Psi = q_e^2\overline{\|\vec{E}\|^2}/2m\Omega^2$, where the overline holds for the average over one rf period. The psp does not obey the superposition theorem and in our case of superimposed rf fields, the resulting psp writes as :

$$\Psi\left(\mathcal{R},\phi\right) \;=\; \Psi_8(\mathcal{R}) + \Psi_4(\mathcal{R}) + 2\sqrt{\Psi_8(\mathcal{R})\Psi_4(\mathcal{R})}\;\cos\left(2\phi\right) \tag{6}$$

where the $\Psi_{2k}(\mathcal{R})$ are the usual $2k$-polar psp, $2k$ being the number of electrodes [5]:

$$\Psi_{2k}\left(\mathcal{R}\right) = \frac{k^2}{4}\frac{q_e^2 V_{2k}^2}{m\; r_0^2\;\Omega^2}\;\mathcal{R}^{2k-2} = \psi_{2k}\;\mathcal{R}^{2k-2}. \tag{7}$$

By definition of the psp, the pseudo-potential wells exactly match the nodes of the rf electric field. Eq. 6 shows that two extra psp minima, compared to the simple $\Psi_8$ case, are expected for $\mathcal{R} \neq 0$ if $\cos(2\phi) = -1$.

However, the total effective trapping potential $U_{\rm trp}$ responsible for the ion confinement results from the psp itself and the static potential required to trap along the symmetry axis $Oz$ and which can be approximated by a harmonic confinement $m\omega_z^2 z^2/2$. To obey the Laplace equation, this trapping potential has a de-confining counterpart $-m\omega_z^2 r^2/4$ which must be taken into account [8, 11]. In the case of an extra static octupole potential $V_{\rm st}$ applied to the electrodes, the effective trapping potential now reads

$$U_{\rm trp} = \Psi + q_e V_{\rm st}\mathcal{R}^4\cos\left(4\phi\right) + \frac{1}{2}\,m\,\omega_z^2\left(z^2 - \frac{\mathcal{R}^2}{2}r_0^2\right) \tag{8}$$

To make sure that the total potential minima still match the rf field-free positions, it is mandatory to compensate the radial de-confining force by an appropriate choice of the static potential $V_{\rm st}$. The matching of these two forces at the field free positions $(\mathcal{R}_{0\rm f}, \phi_{\pm 1})$ is obtained under the condition:

$$q_e V_{\rm st} = m\;\omega_z^2\;r_0^2\;/\;8\mathcal{R}_{0\rm f}^2 \tag{9}$$

To remain as general as possible, we have considered the extra octupole static voltage to compensate for the de-confining effect of the axial confinement. The use of a quadrupole voltage leads to a similar condition which theoretically does not depend on $\mathcal{R}_{0\rm f}$ (cf. discussion of the realization below). We would like to point out that the rf field cancellation condition Eq. 5 as well as the matching condition Eq. 9 do not depend on the mass of the trapped particles and the process described here can apply to a multi-species system (because $\omega_z^2 \propto 1/m$).

The lowest order expansion of the effective trapping potential around its minima $(\mathcal{R}_{0\rm f}, \phi_{\pm 1})$ allows the definition of characteristic frequencies for the motion in the radial and angular directions, if Eq. 9 is satisfied :

$$\omega_r^2 = \omega_z^2\;\left[\frac{8\psi_4}{m\;r_0^2\;\omega_z^2}\;+1\right] = 4\omega_u^2 + \omega_z^2, \tag{10}$$

$$\omega_\phi^2 = \omega_z^2\;\left[\frac{8\psi_4}{m\;r_0^2\;\omega_z^2}\;-2\right] = 4\omega_u^2 - 2\omega_z^2, \tag{11}$$

where $\omega_u$ is the frequency of motion in the radial plane, when only the rf quadrupole potential is applied. The local steepness of the potential, given in Eq. 10 and 11, is controlled by the quadrupole potential $V_4$ and the axial confinement $\omega_z$, thus ruling the morphology of a cold sample in the local 3D anisotropic harmonic potential $(\omega_r, \omega_\phi, \omega_z)$ [12–14]. A close look at Eq. 11 shows that it takes $q_e V_4 > m r_0^2 \omega_z \Omega/2$ to reach this local 3D harmonic confinement. The local potential being independent of the octupole potential $V_8$, this last parameter can be tuned to independently control the distance between the two minima.

In a second step, we show that ions can effectively be cooled to the Doppler limit and localized in the two extra minima in a controlled manner. For this purpose we carry out m.d. simulations of a set of 10 calcium ions, Doppler laser-cooled along the three directions of space in an octupole trap. The m.d procedure for laser cooling takes into account the absorption and emission processes of photons on the involved atomic transitions. Details of its modeling as well as the definition of temperature used are explained in [14]. The rf electric fields obey Eq. 3 and 4 and at $t = 0$, the rf quadrupole potential $V_4$ and the static octupole potential $V_{\rm st}$ are off. The amplitude of the rf octupole potential $V_8$ is such that cold ions form a $\sim 20$ $\mu$m radius ring in the $z = 0$ plane for $\omega_z = 2\pi \times 1$ MHz, shown on figure 2a. The stability of such a structure has been studied elsewhere [8, 15], where it is shown that the Doppler limit can be reached for the motion along the longitudinal direction and that the cooling of the motion in the radial plane is limited by rf heating [8]. At $t = 2$ ms, the rf amplitude $V_4$ is switched on, breaking the cylindrical symmetry of the trapping potential and producing the separation of the ring in two sets of five ions, as shown on Fig. 2b. From $t = 2$ ms to $t = 4.4$ ms, the amplitude $V_4$ is linearly increased, increasing the distance between the two sets of ions and the steepness of the local potential to reach a separation of $0.22 r_0$. For $t = 4.4$ ms, the ions form two

strings along the z-axis (Fig. 2c and Fig. 2d). At this time, $V_4$ is kept unchanged and $V_{\rm st}$ is switched on from 0 to the value fulfilling Eq. 9 (1.7 V) in 1 ms, matching the equilibrium positions of the strings of ions and the field-free positions and reaching characteristic frequencies $\omega_r = 2\pi \times 4.2$ MHz and $\omega_\phi = 2\pi \times 3.8$ MHz. The signature of this position matching is the abrupt drop of $T_y$, the temperature of the motion along $Oy$, from 0.1 K to the Doppler limit (see Fig. 2e).

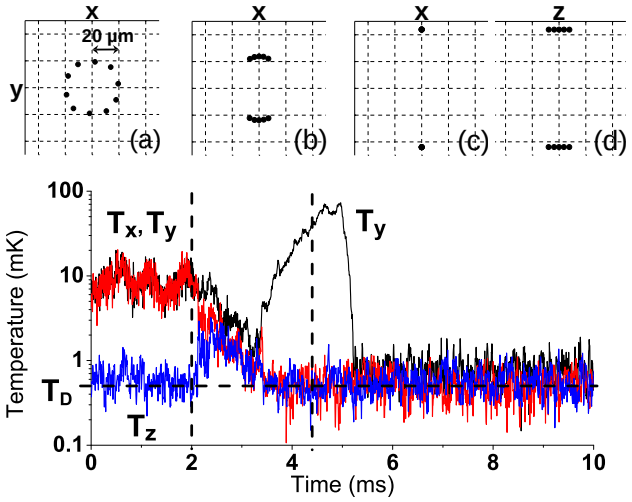


FIG. 2. (Color online) (a)-(d) Pictures of the ion structure at 3 different times (roughly corresponding to the temperature graph below). (e) Temperatures of the different directions of motion for a simulated dynamics detailed in the text. The horizontal dashed line shows the Doppler limit temperature for calcium ions and the vertical dashed lines materialize first, when the quadrupole potential is switched on and second, when the static octupole potential is switched on.

Another signature of this position matching and of the interest of this new ion organization is the lack of rf-heating observed in the simulations when the cooling lasers are switched off, once the parallel lines are formed. Furthermore, tuning the amplitude $V_8$ and the static potential $V_{\rm st}$ accordingly, the ion strings can be moved along the $Oy$ axis. This relative position tuning can be performed with very limited heating as long as the Coulomb repulsion between the two chains is negligible. When it is not the case, this repulsion has to be incorporated in the force compensation condition and a larger static voltage than the one given in Eq. 9 is required.

It is possible to generalize the concept introduced previously. We now assume a $2k$-pole linear trap on which an rf potential $V_{2k}$ is applied. An additional $V_{2p}$ rf potential with identical frequency and phase is superimposed on $2p$ electrodes to generate a rf contribution with a $p$-order of rotational symmetry. Each rf contribution builds its own psp $\Psi_{2k}$ and $\Psi_{2p}$ (see Eq. 7) and the resulting psp can be written as :

$$\Psi = \Psi_{2k} + \Psi_{2p} + 2\sqrt{\Psi_{2k}\Psi_{2p}}\,\cos\left((k-p)\,\phi\right). \qquad (12)$$

The extra psp minima created by cancellation of the rf electric fields are located where $\phi_n = (2n+1)\pi/(k-p)$ (for $\cos((k-p)\phi) = -1$) and $\mathcal{R} = \mathcal{R}_{0\rm f}$ such that

$$\mathcal{R}_{0\rm f}^{k-p} = pV_{2p}/kV_{2k}. \qquad (13)$$

To compensate for the deconfining contribution of the axial confinement at the psp minima, an additional static potential with a $2\pi/(k-p)$ rotational symmetry is required to produce the same confining contribution along all the $\phi_n = (2n+1)\pi/(k-p)$ lines. Depending on the choice of $k$ and $p$, this extra static potential may have a different order of symmetry but a cancellation condition equivalent to Eq. 9 can always be found. As an example, four parallel strings can be formed by the superimposition of an rf quadrupole potential to an rf dodecapole potential, their location match the rf-field nodes providing a static voltage with an octupole symmetry is applied (see figure 3 for different configurations). The order of

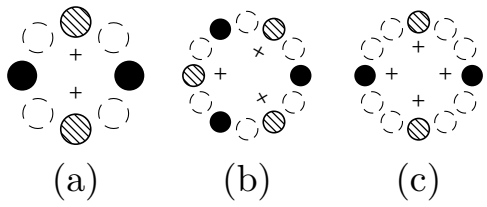


FIG. 3. Diagram of the rf cylindrical rods of different traps where the filled and hatched rods are, respectively, the additional $-V_{2p}$ and $+V_{2p}$ at $t = 0$. Inner crosses stand for the extra field-free positions of (a) octupole trap with additional quadrupole potential, (b) dodecapole trap with hexapole potential, and (c) dodecapole trap with quadrupole potential.

symmetry $s$ of the static potential $V_{st}$ must be a multiple of $(k-p)$. For the case introduced in the first part of this letter, we used $s = 2(k-p) = 4$. This choice has an influence on the characteristic frequencies of the motion of the ions in the extra minima. Indeed, a lowest order expansion of the total trapping potential around these positions results in frequency expressions which are generalizations of Eq. 10 and 11 :

$$\omega_r^2 = 2\,(k-p)^2\,\frac{\psi_{2p}}{m\,r_0^2}\,\mathcal{R}_{0\rm f}^{2p-4} + (s-2)\,\frac{\omega_z^2}{2}, \qquad (14)$$

$$\omega_\phi^2 = 2\,(k-p)^2\,\frac{\psi_{2p}}{m\,r_0^2}\,\mathcal{R}_{0\rm f}^{2p-4} - s\,\frac{\omega_z^2}{2}. \qquad (15)$$

The choice of an order $s$ higher than strictly required by the rotational symmetry may then be justified by the need for high frequencies $\omega_r$ compared to $\omega_\phi$, which can be used to control the morphology of the subsystems (string, zig-zag...) , at the expense of the static voltage itself, which scales as $1/(s\mathcal{R}_{0\rm f}^{s-2})$.

Until now, we have assumed equations for the rf electric field and its psp which correspond to the ideal case of perfectly machined electrodes. Even if the trap design is as ideal as possible, it can not be ideal for both

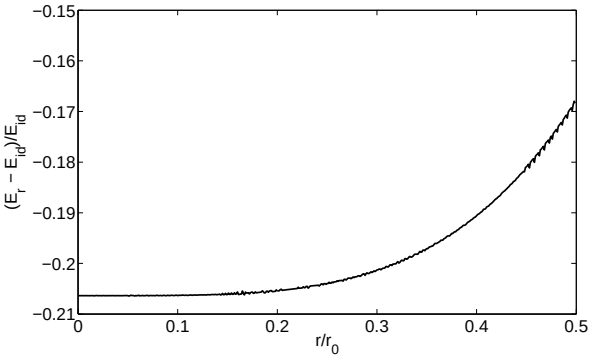


FIG. 4. Normalized difference of the quadrupole electric field, $E_r$, and the ideal one, $E_{id}$, along the radial direction under the angle $\phi_{\pm 1}$.

the highest and the lowest order potential at the same time. To illustrate such an effect, let us go back to our first example of an extra quadrupole potential applied to the octupole trap electrodes and let's assume the linear octupole trap has round electrodes designed to generate an rf electric field as close as possible as the ideal equation [16]. On the quadrupole point of view, these electrodes are too small to produce an ideal quadrupole field inside the trap [9] and most importantly, the four non-connected electrodes are equivalent to grounded rods which induce a large deviation from the ideal rf field. Using SIMION software [17], we have calculated the potential created by a quadrupole-like voltage connection on the octupole trap used for the previous m.d. simulations. Its relevant characteristics are an inner radius of $r_0 = 0.2$ mm and an electrode radius of $r_0/3$, which corresponds to the optimisation of the octupole potential [16]. The calculation shows that the actual quadrupole potential deviates from the ideal one but keeps the quadrupole symmetry. In figure 4 is drawn the normalized difference of the actual quadrupole field component $E_r$ with respect to the ideal one, $E_{id}$, along the radial direction under the angle $\phi_{\pm 1}$. This value is constant in the central part of the trap ($r < r_0/5$) where, providing an $E_r$ amplitude 20% higher, the fields can be considered identical. As an example, the ion ring in Figure 2 fills a tenth of the actual trap dimensions. Figure 4 also shows that Eq. 9 becomes position-dependent for an extra quadrupole static voltage, and thus justifies the use of the optimized static octupole voltage if more distant positions were required.

The m.d. simulations using the calculated potential, fitted by a polynomial equation [18] show that the same procedure to create two strings, to bring them to the rf nodes and to laser cool them to the Doppler limit can be performed.

We have shown that a superimposed lower-order rf potential onto the main trapping one adds supplementary nodes in the rf field. An ensemble of ions can be separated in several sub-sets in a controlled manner and laser-cooled to the Doppler limit. Once cooled, they can be considered as in a 3D anisotropic harmonic potential and controlled like in a linear quadrupole trap. This opens the way to create parallel ion strings with a large choice of geometries. The distance between the potential minima can be continuously tuned to reach conditions where the Coulomb repulsion between the subsets implies a strong enough correlation to influence their relative equilibrium positions. The different patterns formed by neighboring ions seem specifically interesting for quantum simulations [19, 20], but may certainly find interesting applications in other domains.


[1] A. L. Wolf, S. A. van den Berg, W. Ubachs, and K. S. E. Eikema, Phys. Rev. Lett. **102**, 223901 (Jun 2009).
[2] C. W. Chou, D. B. Hume, J. C. J. Koelemeij, D. J. Wineland, and T. Rosenband, Phys. Rev. Lett. **104**, 070802 (Feb 2010).
[3] R. Blatt and D. Wineland, Nature **453**, 1008 (2008).
[4] M. Johanning, A. F. Varon, and C. Wunderlich, J. Phys. B: At. Mol. Opt. Phys. **42**, 154009 (2009).
[5] D. Gerlich, "Inhomogeneous rf fields: a versatile tool for the study of processes with slow ions," (John Wiley and Sons, 1992).
[6] J. Prestage, R. Tjoelker, and L. Maleki, Proceedings of the 1999 Joint EFTF-IFCS, Besancon, France, 121(1999).
[7] R. Wester, J. Phys. B: At. Mol. Opt. Phys. **42**, 154001 (2009).
[8] C. Champenois, M. Marciante, J. Pedregosa-Gutierrez, M. Houssin, M. Knoop, and M. Kajita, Phys. Rev. A **81**, 043410 (Apr 2010).
[9] A. J. Reuben, G. B. Smith, P. Moses, A. V. Vagov, M. D. Woods, D. B. Gordon, and R. W. Munn, Int. J. Mass Spectrom. **154**, 43 (1996).
[10] H. Dehmelt, Adv. At. Mol. Phys. **3**, 53 (1967).
[11] M. Drewsen and A. Brøner, Phys. Rev. A **62**, 045401 (2000).
[12] J. P. Schiffer, Phys. Rev. Lett. **70**, 818 (Feb 1993).
[13] D. Dubin, Physics of Fluids B **5**, 295 (1993).
[14] M. Marciante, C. Champenois, A. Calisti, J. Pedregosa-Gutierrez, and M. Knoop, Phys. Rev. A **82**, 033406 (2010).
[15] K. Okada, K. Yasuda, T. Takayanagi, M. Wada, H. A. Schuessler, and S. Ohtani, Phys. Rev. A **75**, 033409 (2007).
[16] A. Konenkov, D. Douglas, and N. Konenkov, Int. J. Mass Spectrom. **289**, 144 (2010).
[17] http://www.simion.com.
[18] J. Pedregosa, C. Champenois, M. Houssin, and M. Knoop, Int. J. Mass Spectrom. **290**, 100 (2010).
[19] I. Buluta and F. Nori, Science **326**, 108 (2009).
[20] G. K. Brennen, M. Aguado, and J. I. Cirac, New J. Phys. **11**, 053009 (2009).